Persistent vibrational structure in $^{110–116}$Cd

N. Gavrielov [1,2,*] J. E. García-Ramos [3,†] P. Van Isacker [4,‡] and A. Leviatan [2,§]

[1]*Center for Theoretical Physics, Sloane Physics Laboratory, Yale University, New Haven, Connecticut 06520-8120, USA*

[2]*Racah Institute of Physics, The Hebrew University, Jerusalem 91904, Israel*

[3]*Department of Integrated Sciences and Center for Advanced Studies in Physics, Mathematics and Computation,*
University of Huelva, 21071 Huelva, Spain

[4]*Grand Accélérateur National d'Ions Lourds, CEA/DRF-CNRS/IN2P3, Bvd Henri Becquerel, BP 55027, F-14076 Caen, France*

The empirical spectra and $E2$ decay rates in ^{110,112,114,116}Cd are shown to be consistent with a vibrational interpretation for low-lying normal states, coexisting with a single deformed γ-soft band of intruder states. The observed deviations from this paradigm show up in particular nonyrast states, which are properly described by a Hamiltonian with U(5) partial dynamical symmetry. The latter is characterized by a good (broken) symmetry in most (in selected) normal states, weakly coupled to intruder states.

The concepts of shapes and symmetries play a pivotal role in the quest for understanding the structure and simple patterns in complex many-body systems. A notable example is found in atomic nuclei, where these notions are instrumental for interpreting the collective motion exhibited by a multitude of protons and neutrons subject to the strong interaction. Based on earlier ideas of Bohr and Kalckar [1,2] and on Rainwater's suggestion [3] that nuclei may be intrinsically deformed, a standard description of the nucleus was proposed in terms of a quantum liquid drop, which can vibrate and, if deformed, also rotate. This is commonly referred to as the (Bohr-Mottelson) collective model of the nucleus [4–6]. Particular limits of the model provide insightful paradigms for the dynamics of spherical, axially deformed, and non-axial shapes. These geometric benchmarks correspond in the algebraic interacting boson model (IBM) of Arima and Iachello [7] to solvable limits, associated with dynamical symmetries.

Recent advances in high resolution spectroscopy of nonyrast states [8], impart valuable input for testing and challenging the accepted paradigms of collective motion in nuclei. The present work examines the collective model hypothesis of quadrupole oscillations about a spherical shape, in relation to the cadmium isotopes ($Z = 48$). The latter have long since been considered as textbook examples of spherical-vibrator nuclei and U(5) dynamical symmetry [6,7,9–11]. On the other hand, detailed studies, using complementary spectroscopic methods, have provided evidence for marked deviations from such a structural paradigm [12–17]. Two approaches have been proposed to address these unexpected findings. The first questions the spherical-vibrational character of the ^{110,112}Cd

isotopes, replacing it with multiple coexistence of states with different deformed shapes in the same nucleus, a view qualitatively supported by a beyond-mean-field (BMF) calculation with the Gogny D1S energy density functional [18,19]. A second approach is based on the recognition that the reported deviations from a spherical-vibrator behavior show up in selected states, while most states retain their vibrational character. In the terminology of symmetry, this implies that the symmetry in question is broken only in a subset of states, hence is partial [20]. Such a U(5) partial dynamical symmetry (PDS) approach was applied in Ref. [21] to describe the properties of ^{110}Cd.

In this Letter, it is shown that the U(5)-PDS approach of Ref. [21] can be extended to give a coherent description of a *series* of cadmium isotopes with mass number $A = 110$–116. Their properties are analyzed based on a vibrational interpretation coupled to the presence of intruder states. It is by now widely accepted that the Cd isotopes exhibit shape coexistence in their low-energy spectrum [22–25]. However, unlike the multishape version of coexistence in Refs. [18,19], only two coexisting configurations with different shapes are proposed here: a spherical one, exhibiting an anharmonic vibrational spectrum for normal states, and one that is prolate deformed with γ-soft characteristics, that is, an axially symmetric shape that can easily turn triaxial, for intruder states. The anharmonicity is due to the presence of terms in the Hamiltonian that break the U(5) symmetry in selected normal states, and is essential to reproduce the unexpected observed $E2$ decay patterns. In this respect, it should be mentioned that previous attempts to explain the experimental $E2$ matrix elements relied on strong mixing between spherical and intruder states and ultimately proved unsuccessful [12–16,26,27].

Vibrations of spherical nuclei can be described in the U(5) dynamical symmetry (DS) limit of the IBM, associated with the chain, U(6) ⊃ U(5) ⊃ SO(5) ⊃ SO(3). The DS basis states $|[N], n_d, \tau, n_\Delta, L\rangle$ have quantum numbers which are the labels of irreducible representations of the algebras in

*noam.gavrielov@yale.edu

†enrique.ramos@dfaie.uhu.es

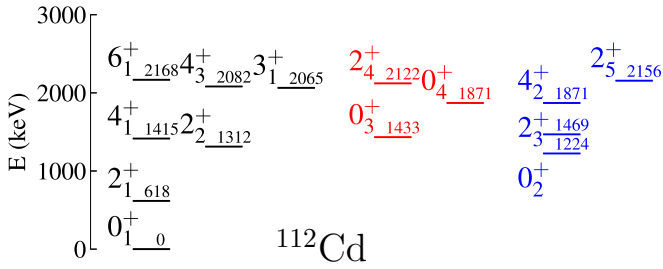‡isacker@ganil.fr

§ami@phys.huji.ac.il

FIG. 1. Experimental energy levels in keV of ^{112}Cd [28]. Normal states are marked in black or in red if their $E2$ decays deviate from those of a spherical vibrator. Intruder states are marked in blue.

the chain. Here, N is the total number of monopole (s) and quadrupole (d) bosons, n_d and τ are the d-boson number and seniority, respectively, L is the angular momentum, and n_Δ is a multiplicity label. The U(5)-DS Hamiltonian can be transcribed in the form

$$\hat{H}_{\rm DS} = \rho_1 \hat{n}_d + \rho_2 \hat{n}_d(\hat{n}_d - 1) + \rho_3[-\hat{C}_{\rm SO(5)} + \hat{n}_d(\hat{n}_d + 3)]$$
$$+ \rho_4[\hat{C}_{\rm SO(3)} - 6\hat{n}_d], \quad (1)$$

where $\hat{C}_G$ denotes a Casimir operator of G, and $\hat{n}_d = \sum_m d_m^\dagger d_m = \hat{C}_{\rm U(5)}$. $\hat{H}_{\rm DS}$ is completely solvable with eigenstates $|[N], n_d, \tau, n_\Delta, L\rangle$ and energies $E_{\rm DS} = \rho_1 n_d + \rho_2 n_d (n_d - 1) + \rho_3 (n_d - \tau)(n_d + \tau + 3) + \rho_4[L(L+1) - 6n_d]$. The U(5)-DS spectrum is that of a spherical vibrator with states arranged in n_d multiplets, the lowest ones being $(n_d = 0, L = 0)$, $(n_d = 1, L = 2)$, $(n_d = 2, L = 4, 2, 0)$, $(n_d = 3, L = 6, 4, 3, 0, 2)$ at energies $E(n_d) \approx n_d E(n_d = 1)$. The $E2$ operator in the IBM is proportional to

$$\hat{Q}_\chi = d^\dagger s + s^\dagger \tilde{d} + \chi(d^\dagger \tilde{d})^{(2)}, \quad (2)$$

where $\tilde{d}_m = (-1)^m d_{-m}$. It is customary in the U(5)-DS limit to set $\chi = 0$, which results in vanishing quadrupole moments

and strong $(n_d + 1 \to n_d)$ $E2$ transitions with particular ratios, e.g., $\frac{B(E2; n_d+1, L'=2n_d+2 \to n_d, L=2n_d)}{B(E2; n_d=1, L=2 \to n_d=0, L=0)} = (n_d + 1)\frac{(N-1)}{N}$.

The empirical spectrum of ^{112}Cd, shown in Fig. 1, consists of both normal and intruder levels, the latter based on 2p-4h proton excitations across the $Z = 50$ shell gap. At first sight, the normal states seem to follow the expected pattern of spherical-vibrator n_d multiplets. The measured $E2$ rates support this view for the majority of normal states, however, selected nonyrast states (shown in red in Fig. 1) reveal marked deviations from this behavior. Specifically, the 0_3^+ and 2_4^+ states in ^{112}Cd (denoted in Table I by 0_α^+ and 2_α^+) which in the U(5)-DS classification are members of the $n_d = 2$ and $n_d = 3$ multiplets, respectively, have unusually small $E2$ rates for the transitions $0_\alpha^+ \to 2_1^+$ and $2_\alpha^+ \to 2_2^+$, and large rates for $0_\alpha^+ \to 2_2^+$, at variance with the U(5)-DS predictions. Absolute $B(E2)$ values for transitions from the 0_4^+ state are not known, but its branching ratio to the 2_2^+ state is small. As shown in Table I, the same unexpected decay patterns occur in all $^{110-116}$Cd isotopes and comprise the so-called "Cd problem" [25]. We are thus confronted with a situation in which some states in the spectrum obey the predictions of U(5)-DS, while other states do not. These empirical findings suggest the presence of a PDS, as demonstrated for ^{110}Cd in [21]. In what follows, we show that the same U(5)-PDS approach is relevant also to the other Cd isotopes.

To describe both normal and intruder states, we adopt the interacting boson model with configuration mixing (IBM-CM) [29,30], widely used to study shape coexistence in nuclei [31–35]. The Hamiltonian is written as

$$\hat{H} = \hat{H}_{\rm PDS}^{(N)} + \hat{H}_{\rm intrud}^{(N+2)} + \hat{V}_{\rm mix}^{(N,N+2)}, \quad (3)$$

where the superscript (N) denotes a projection onto a space of N bosons. Here, $\hat{H}_{\rm PDS}^{(N)}$ represents the normal configuration (N boson space), $\hat{H}_{\rm intrud}^{(N+2)}$ represents the intruder configuration

TABLE I. Experimental (EXP) $B(E2)$ values in Weisskopf units (W.u.) and quadrupole moments $Q(2_1^+)$ in eb, for normal levels in $^{110-116}$Cd, compared to calculated U(5)-DS and PDS values. The 0_α^+ (2_α^+) state corresponds to the experimental $0_3^+, 0_3^+, 0_3^+, 0_2^+$ ($2_5^+, 2_4^+, 2_5^+, 2_4^+$) state for ^{A}Cd ($A = 110, 112, 114, 116$), respectively. In the U(5)-DS classification, $(0_1^+, 2_1^+, 2_2^+, 4_1^+, 6_1^+)$ are class-A states with $n_d = 0, 1, 2, 2, 3$ and $(0_\alpha^+, 2_\alpha^+)$ are states with $n_d = (2, 3)$. The U(5)-PDS calculations are obtained using $\hat{T}(E2)$, Eq. (6), with parameters given in Fig. 2. Data are taken from [12,15–17,28].

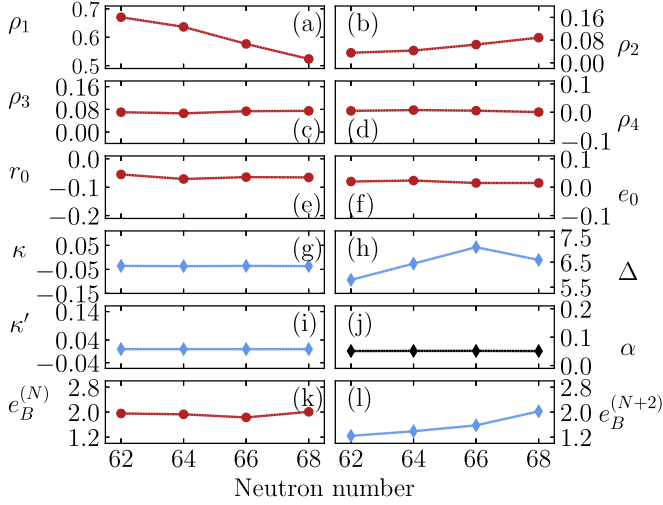|		^{110}Cd			^{112}Cd			^{114}Cd			^{116}Cd		
L_i	L_f	EXP	U(5)-DS	PDS	EXP	U(5)-DS	PDS	EXP	U(5)-DS	PDS	EXP	U(5)-DS	PDS
2_1^+	0_1^+	27.0(8)	27.0	27.0	30.31(19)	30.31	30.31	31.1(19)	31.1	31.1	33.5(12)	33.5	33.5
4_1^+	2_1^+	42(9)	46	46	63(8)	53	52	62(4)	55	55	56(14)	59	60
2_2^+	2_1^+	30(5)	46	45	39(7)	53	51	22(6)	55	53	25(10)	59	59
2_2^+	0_1^+	0.68(14)	0	0.0	0.65(11)	0	0.0	0.48(6)	0	0.0	1.11(18)	0	0.0
6_1^+	4_1^+	40(30)	58	53		68	59	119(15)	72	70	110^{+40}_{-80}	75	79
0_α^+	2_1^+	<7.9	46	0.08	0.0121(17)	53	0.01	0.0026(4)	55	0.0026	0.79(22)	59	0.79
0_α^+	2_2^+	<1680	0	43	99(16)	0	49	127(16)	0	61		0	60
2_α^+	2_2^+	$0.7^{+0.5}_{-0.6}$	11	0.124	$<1.6^{+6}_{-4}$	13	0.08	2.5^{+16}_{-14}	14	0.005	2.0(6)	14	0.004
2_α^+	0_α^+	24.2(22)	27	21	25(7)	32	28	17(5)	34	33	35(10)	35	33
$Q(2_1^+)$		−0.40(3)	0	−0.13	−0.38(3)	0	−0.13	−0.35(5)	0	−0.13	−0.42(4)	0	−0.14

FIG. 2. Parameters of the IBM-CM Hamiltonian, Eq. (3), in MeV and of the $E2$ operator, Eq. (6), with $e_B^{(N)}$, $e_B^{(N+2)}$ in $\sqrt{\text{W.u.}}$ and $\chi_n = -0.7$, $\chi = -0.09$ are dimensionless. The boson numbers in the (normal, intruder) configurations are $(N, N+2)$ with $N = 7, 8, 9$ and $\bar{N} = 8$ (hole bosons) for neutron numbers 62, 64, 66, and 68, respectively.

($N+2$ boson space), and $\hat{V}_{\text{mix}}^{(N,N+2)}$ a mixing term. Explicit forms are given by

$$\hat{H}_{\text{PDS}} = \hat{H}_{\text{DS}} + r_0\, G_0^\dagger G_0 + e_0\, (G_0^\dagger K_0 + K_0^\dagger G_0), \quad (4a)$$

$$\hat{H}_{\text{intrud}} = \kappa \hat{Q}_\chi \cdot \hat{Q}_\chi + \kappa' \hat{L} \cdot \hat{L} + \Delta, \quad (4b)$$

$$\hat{V}_{\text{mix}} = \alpha[(s^\dagger)^2 + (d^\dagger d^\dagger)^{(0)}] + \text{H.c.}, \quad (4c)$$

where $\hat{H}_{\text{DS}}$ is the U(5)-DS Hamiltonian of Eq. (1), $G_0^\dagger = [(d^\dagger d^\dagger)^{(2)} d^\dagger]^{(0)}$, $K_0^\dagger = s^\dagger (d^\dagger d^\dagger)^{(0)}$, $\hat{Q}_\chi$ is given in Eq. (2), and H.c. means Hermitian conjugate. As shown in [21], $\hat{H}_{\text{PDS}}$ has U(5)-PDS in the sense that it breaks the U(5) symmetry, yet maintains a subset of U(5)-DS basis states $|n_d = \tau, \tau, n_\Delta = 0, L\rangle$ with $L = \tau, \tau + 1, \ldots, 2\tau - 2, 2\tau$, as solvable eigenstates. Henceforth, we refer to this special subset of states as class-A states. The eigenstates $|\Psi; L\rangle$ of $\hat{H}$, Eq. (3), involve normal (Ψ_n) and intruder (Ψ_i) components in the [N] and [$N + 2$] boson spaces,

$$|\Psi; L\rangle = a\, |\Psi_n; [N], L\rangle + b\, |\Psi_i; [N + 2], L\rangle \quad (5)$$

with $a^2 + b^2 = 1$. The $E2$ operator in the IBM-CM reads

$$\hat{T}(E2) = e_B^{(N)} \hat{Q}_{\chi_n}^{(N)} + e_B^{(N+2)} \hat{Q}_\chi^{(N+2)} \quad (6)$$

with boson effective charges $e_B^{(N)}$ and $e_B^{(N+2)}$.

The parameters of $\hat{H}$ (3) and $\hat{T}(E2)$ (6) are determined by a combined fit to the spectra and $E2$ transitions for the normal states $(2_1^+, 4_1^+, 2_2^+, 6_1^+)$ and $(0_\alpha^+, 2_\alpha^+)$, and for the lowest $(0^+, 2^+)$ intruder states in each isotope. As shown in Fig. 2, the extracted parameters are fairly constant and vary smoothly as a function of neutron number. Notable exceptions are ρ_1 whose decrease reflects the lowering of the 2_1^+ state, and Δ, which together with the κ term in $\hat{H}_{\text{intrud}}$ controls the lowering of the intruder levels towards midshell (neutron number 66), where boson particles are replaced by boson holes.
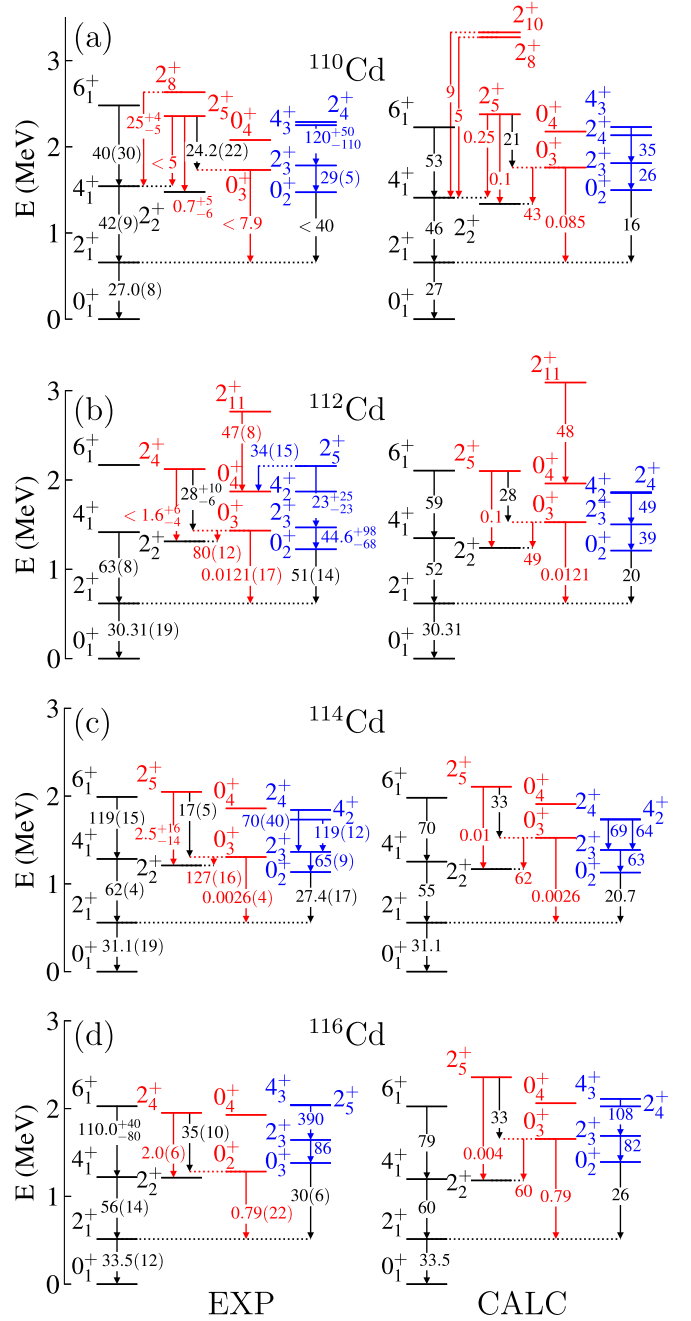

FIG. 3. Comparison between selected experimental (left panels) and calculated (right panels) energy levels in MeV and $E2$ transition rates in W.u.

An IBM-CM calculation has been performed for spectral properties of states in $^{110-116}$Cd, with energies up to 4 MeV. A detailed account will be given in a forthcoming longer publication [36]. Here, we focus on the main features which are relevant to the subject matter of this Letter, namely, the vibrational interpretation and symmetry aspects of these isotopes. The assignment of states as normal or intruder is based on their measured $E2$ decays when available, or on their calculated probabilities, a^2 and b^2, in Eq. (5).

TABLE II. Normal-intruder mixing and U(5) structure of the wave functions $|\Psi, L\rangle$, Eq. (5), of selected eigenstates of $\hat{H}$, Eq. (3). Shown are the probability (a^2) of the normal part Ψ_n, the dominant n_d component in Ψ_n and its probability P_{n_d}.

L_k^+	^{110}Cd		^{112}Cd		^{114}Cd		^{116}Cd	
	a^2 (%)	$[(n_d)\, P_{n_d}(\%)]$	a^2 (%)	$[(n_d)\, P_{n_d}(\%)]$	a^2 (%)	$[(n_d)\, P_{n_d}(\%)]$	a^2 (%)	$[(n_d)\, P_{n_d}(\%)]$
0_1^+	98.23	[(0) 98.22]	97.94	[(0) 97.92]	97.98	[(0) 97.95]	98.27	[(0) 98.25]
2_1^+	96.38	[(1) 96.36]	95.10	[(1) 95.05]	95.28	[(1) 95.22]	96.84	[(1) 96.81]
4_1^+	90.73	[(2) 90.69]	83.19	[(2) 83.03]	83.05	[(2) 82.87]	92.95	[(2) 92.91]
2_2^+	89.81	[(2) 89.74]	81.62	[(2) 81.28]	78.77	[(2) 78.33]	91.31	[(2) 91.25]
6_1^+	71.18	[(3) 71.09]	42.92	[(3) 42.53]	39.46	[(3) 38.98]	79.34	[(3) 79.27]
0_α^+	70.75	[(3) 70.46]	71.13	[(3) 69.54]	71.55	[(3) 70.79]	74.34	[(3) 74.14]
2_α^+	68.34	[(4) 66.07]	65.89	[(4) 62.83]	40.78	[(4) 40.13]	55.68	[(4) 54.73]

As shown in Fig. 3 and Table I, the U(5)-PDS calculation of spectra and $E2$ rates provides a good description of the empirical data in $^{110-116}$Cd. It yields the same $B(E2)$ values as those of U(5)-DS for class-A states and reproduces correctly the $E2$ transitions involving the $(0_\alpha^+, 2_\alpha^+)$ states which deviate considerably from the U(5)-DS predictions. The origin of these features is revealed from Table II, which shows for eigenfunctions of $\hat{H}$ Eq. (3), the percentage of the wave function within the normal configuration [the probability a^2 of Ψ_n in Eq. (5)] and the dominant n_d component in Ψ_n and its probability.

The class-A states are dominated by the normal component Ψ_n (large $a^2 \geqslant 90\%$), implying a weak mixing (small b^2) with the intruder states. The 6_1^+ state experiences a larger mixing consistent with its enhanced decay to the lowest 4^+ intruder state. The $(0_\alpha^+, 2_\alpha^+)$ states are more susceptible to such mixing but still retain the dominance of Ψ_n ($a^2 \sim 70\%$). For both types of states the normal-intruder mixing increases with L for a given isotope, and increases towards midshell (^{114}Cd), correlated with the decrease in energy of intruder states.

The class-A states possess good U(5) quantum numbers to a good approximation. Their Ψ_n part involves a single n_d component with probability $P_{n_d} \geqslant 90\%$, as in U(5)-DS. In contrast, the structure of the nonyrast $(0_\alpha^+, 2_\alpha^+)$ states changes dramatically. Specifically, the Ψ_n parts of the 0_α^+ and 2_α^+ states, which in the U(5)-DS classification have $n_d = 2$ and $n_d = 3$, have now dominant components with $n_d = 3$ and $n_d = 4$, respectively. The change $n_d \mapsto (n_d + 1)$ ensures weak ($\Delta n_d = 2$) transitions from these states to class-A states, but secures strong $2_\alpha^+ \to 0_\alpha^+$ ($\Delta n_d = 1$) transitions, in agreement with the data. While the class-A and $(0_\alpha^+, 2_\alpha^+)$ states are predominantly spherical, the intruder states are members of a single deformed band with a characteristic γ-soft spectrum, shown in Fig. 3, and wave functions exhibiting a broad n_d distribution and a pronounced SO(6) symmetry $\sigma = N+2$.

The PDS-CM describes the data very well, but there are a few exceptions and remaining concerns. The observed quadrupole moments $Q(2_1^+)$ and $B(E2; 2_2^+ \to 0_1^+)$, shown in Table I, are larger than the predicted values which, in turn, depend sensitively on the choice of χ_n in Eq. (6). Larger values for these observables (which involve class-A states) can be accommodated by adding U(5) symmetry-breaking terms to the Hamiltonian. The $(0_\alpha^+, 2_\alpha^+)$ states are predominantly $n_d = (3, 4)$. A relevant question [19], is where their partner states with $n_d = (2, 3)$ are with enhanced decays to states with $n_d = (1, 2)$. The observed 0_4^+ state, shown in Fig. 3, has a dominant branching to the intruder 2_3^+ state, hence does not match the properties expected for a $n_d = 2$ state. This may indicate a different structure for the 0_4^+ state (e.g., a 4p-6h proton excitation as speculated in [17]), although fragmentation of $E2$ strength cannot be ruled out. In ^{110}Cd, the state $2_8^+(2633)$ has a large $B(E2; 2_8^+ \to 4_1^+) = 25_{-5}^{+4}$ W.u. [28], as expected for a $(n_d = 3) \to (n_d = 2)$ transition. More data are needed to shed light on this issue.

The vibrational interpretation proposed here is at variance with the microscopic BMF calculation of Refs. [18,19] advocating multiple shape coexistence in ^{110,112}Cd with states arranged in deformed rotational bands. Specifically, the states $0_1^+, 2_1^+, 0_3^+, 0_4^+$, of ^{112}Cd, shown in Fig. 1, serve as band heads for the ground, γ and two excited $K=0$ bands, and $0_2^+, 2_5^+$ are band heads for intruder and intruder-γ bands. Similar assignments were suggested for ^{110}Cd. The BMF-based approach is parameter free and provides a qualitative description of ^{110,112}Cd, but with noticeable shortcomings. In particular, the predicted energies are generally overestimated, and inband $B(E2)$ values and quadrupole moments are greater than observed, reflecting too large deformations in the calculated states. A detailed comparison between the BMF-based approach and the current PDS-based approach will be given in [36] with a view that, ultimately, comparison with data should be the basis to accept or refute a model. One possible signature that can distinguish between the two approaches is to measure the value of $B(E2; 4_2^+ \to 3_1^+)$, which is expected to be small (large) in the PDS (BMF) approach, where the indicated states are in the same n_d multiplet (in the same γ band).

To summarize, consistent with the empirical data, we have shown that a vibrational interpretation and good U(5) symmetry are maintained for the majority of low-lying normal states, coexisting with a single deformed band of intruder states in ^{110,112,114,116}Cd isotopes. The observed deviations from this paradigm are properly treated by a Hamiltonian which breaks the U(5) symmetry in selected nonyrast states, while keeping the mixing with intruder states weak. The results demonstrate

the relevance of a partial dynamical symmetry (PDS) to a series of isotopes, and set the path for implementing a similar PDS-based approach to other regions of the nuclear chart, where a prescribed collective structure paradigm holds for a segment of the spectrum.

[1] N. Bohr, Nature (London) **137**, 344 (1936).

[2] N. Bohr and F. Kalckar, Mat. Fys. Medd. Dan. Vid. Selsk. **14**(10) (1937).

[3] J. Rainwater, Phys. Rev. **79**, 432 (1950).

[4] A. Bohr, Mat. Fys. Medd. Dan. Vid. Selsk. **26**(14) (1952).

[5] A. Bohr and B. R. Mottelson, Mat. Fys. Medd. Dan. Vid. Selsk. **27**(16) (1953).

[6] A. Bohr and B. R. Mottelson, *Nuclear Structure. II Nuclear Deformations* (Benjamin, New York, 1975).

[7] F. Iachello and A. Arima, *The Interacting Boson Model* (Cambridge University Press, Cambridge, 1987).

[8] P. E. Garrett, M. Zielińska, and E. Clément, Prog. Part. Nucl. Phys. **124**, 103931 (2022).

[9] R. F. Casten, *Nuclear Structure from a Simple Perspective* (Oxford University Press, Oxford, 2000).

[10] K. Heyde, *Basic Ideas and Concepts in Nuclear Physics* (Institute of Physics, Bristol, 2004).

[11] D. J. Rowe and J. L. Wood, *Fundamentals of Nuclear Models* (World Scientific, Singapore, 2010).

[12] P. E. Garrett, K. L. Green, H. Lehmann, J. Jolie, C. A. McGrath, M. Yeh, and S. W. Yates, Phys. Rev. C **75**, 054310 (2007).

[13] R. F. Casten, J. Jolie, H. G. Börner, D. S. Brenner, N. V. Zamfir, W.-T. Chou, and A. Aprahamian, Phys. Lett. B **297**, 19 (1992).

[14] M. Kadi, N. Warr, P. E. Garrett, J. Jolie, and S. W. Yates, Phys. Rev. C **68**, 031306(R) (2003).

[15] P. E. Garrett, K. L. Green, and J. L. Wood, Phys. Rev. C **78**, 044307 (2008).

[16] P. E. Garrett and J. L. Wood, J. Phys. G: Nucl. Part. Phys. **37**, 064028 (2010); **37**, 069701 (2010).

[17] P. E. Garrett, J. Bangay, A. Diaz Varela, G. C. Ball, D. S. Cross, G. A. Demand *et al.*, Phys. Rev. C **86**, 044304 (2012).

[18] P. E. Garrett, T. R. Rodríguez, A. D. Varela, K. L. Green, J. Bangay, A. Finlay *et al.*, Phys. Rev. Lett. **123**, 142502 (2019).

[19] P. E. Garrett, T. R. Rodríguez, A. Diaz Varela, K. L. Green, J. Bangay, A. Finlay *et al.*, Phys. Rev. C **101**, 044302 (2020).

[20] A. Leviatan, Prog. Part. Nucl. Phys. **66**, 93 (2011).

[21] A. Leviatan, N. Gavrielov, J. E. García-Ramos, and P. Van Isacker, Phys. Rev. C **98**, 031302(R) (2018).

[22] G. Gneuss and W. Greiner, Nucl. Phys. A **171**, 449 (1971).

[23] H. W. Fielding *et al.*, Nucl. Phys. A **281**, 389 (1977).

[24] J. Kumpulainen, R. Julin, J. Kantele, A. Passoja, W. H. Trzaska, E. Verho, J. Väärämäki, D. Cutoiu, and M. Ivascu, Phys. Rev. C **45**, 640 (1992).

[25] K. Heyde and J. L. Wood, Rev. Mod. Phys. **83**, 1467 (2011).

[26] M. Délèze, S. Drissi, J. Kern, P. A. Ternier, J. P. Vorlet, J. Rikovska, T. Otsuka, S. Judge, and A. Williams, Nucl. Phys. A **551**, 269 (1993).

[27] K. Heyde, P. Van Isacker, M. Waroquier, G. Wenes, and M. Sambataro, Phys. Rev. C **25**, 3160 (1982).

[28] Evaluated Nuclear Structure Data File (ENSDF), https://www.nndc.bnl.gov/ensdf/.

[29] P. D. Duval and B. R. Barrett, Phys. Lett. B **100**, 223 (1981).

[30] P. D. Duval and B. R. Barrett, Nucl. Phys. A **376**, 213 (1982).

[31] J. E. García-Ramos and K. Heyde, Phys. Rev. C **89**, 014306 (2014).

[32] J. E. García-Ramos and K. Heyde, Phys. Rev. C **92**, 034309 (2015).

[33] K. Nomura and J. Jolie, Phys. Rev. C **98**, 024303 (2018).

[34] N. Gavrielov, A. Leviatan, and F. Iachello, Phys. Rev. C **105**, 014305 (2022).

[35] E. Maya-Barbecho and J. E. García-Ramos, Phys. Rev. C **105**, 034341 (2022).

[36] N. Gavrielov, P. Van Isacker, J. E. García-Ramos, and A. Leviatan (to be published).